Continuous-variable telecloning with phase-conjugate inputs

Jing Zhang,* Changde Xie, and Kunchi Peng
State Key Laboratory of Quantum Optics and Quantum Optics Devices, Institute of Opto-Electronics, Shanxi University, Taiyuan 030006, People's Republic of China

Peter van Loock
Optical Quantum Information Theory Group, Institute of Theoretical Physics I and Max-Planck Research Group, Institute of Optics, Information and Photonics, Universität Erlangen-Nürnberg, Staudtstrasse 7/B2, 91058 Erlangen, Germany
(Received 21 November 2007; published 14 February 2008)

We propose a scheme for continuous-variable telecloning with phase-conjugate inputs (PCI). Two cases of PCI telecloning are considered. The first case is where PCI telecloning produces M clones nonlocally and M anticlones locally, or vice versa. This kind of PCI telecloning requires only one Einstein-Podolsky-Rosen (EPR) entangled, two-mode squeezed state as a resource for building the appropriate multimode, multipartite entangled state via linear optics. The other case is a PCI telecloning protocol in which both clones and anticlones are created nonlocally. Such a scheme requires two EPR entangled states for the generation of a suitable multipartite entangled state. As our schemes are reversible, optimal cloning fidelities are achieved in the limit of infinite squeezing.

DOI: 10.1103/PhysRevA.77.022316 PACS number(s): 03.67.Hk, 03.67.Mn, 42.50.Lc

I. INTRODUCTION

Arbitrary quantum states cannot be copied perfectly according to the quantum mechanical no-cloning theorem [1,2]. However, there are optimal quantum cloning protocols that lead to imperfect, approximate copies resembling the input state just as much as allowed by quantum theory. This quantum cloning plays an important role in quantum information and quantum communication. For instance, it has been shown that quantum cloning might improve the performance of some computational tasks [3]. Quantum cloning also represents a potential eavesdropping attack in quantum cryptographic protocols [4].

An approximate, optimal quantum cloning machine was first considered by Bužek and Hillery [5]. Their cloner operates in the domain of discrete variables and acts upon qubit states. Later, quantum cloning was extended to the continuous-variable (CV) regime by Cerf *et al.* [6]. Continuous-variable quantum cloning has been extensively studied in recent years. This interest has been partly motivated by the fact that preparing and manipulating optical, Gaussian, CV quantum states is relatively easy compared to other implementations. There are various theoretical proposals for an experimental realization of CV quantum cloning [7–9]. These first proposals rely upon linear optics and, in addition, on the optical amplification of the input states. The cloned states in these schemes are produced locally, from a number of identical copies of the signal state. We refer to this kind of quantum cloning as local, conventional cloning. A more recent experimental realization of local, conventional cloning of optical coherent states was achieved without amplification, using only linear optics, homodyne detection, and feedforward [10]. According to another interesting proposal of this kind of cloning [11], approximate copies of an optical quantum state appear in two atomic ensembles.

There has also been a lot of interest in quantum nonlocal cloning (telecloning), which is a combination of quantum cloning and teleportation to more than just one receiver. The aim of telecloning is to broadcast information of an unknown quantum state from a sender to several spatially separated receivers exploiting multipartite entanglement as a multiuser quantum channel. For continuous variables, the first proposal for optimal $1 \rightarrow M$ telecloning of coherent states is based upon an $M+1$ partite entangled multimode Gaussian state [12]. The protocol itself, similar to one-to-one quantum teleportation [13], uses beam splitters, homodyne detection, and feedforward. In this case, the anticlones (phase-conjugate clones, or time-reversed state) are lost; thus, optimal telecloning can be achieved by exploiting nonmaximum, effectively bipartite entanglement produced from finitely squeezed light via linear optics. This scheme (see also [14,15]) is regarded as the CV irreversible telecloner, analogous to the irreversible telecloner in the domain of discrete variables [16]. Recently, irreversible telecloning of optical coherent states was demonstrated experimentally [17].

In addition, CV reversible telecloning was proposed [18], in which the information of an unknown quantum state is, in principle, transferred without loss from a sender to several spatially separated receivers, again exploiting multipartite entanglement as a multiuser quantum channel. However, in this case, optimal reversible telecloning requires maximum bipartite entanglement; hence infinite squeezing would be needed to build the corresponding multimode entangled state [12].

An important work on quantum state estimation has revealed that more quantum information can be encoded in antiparallel pairs of spins than in parallel pairs [19]. Subsequently, a similar result was obtained in the CV regime, where a pair of conjugate Gaussian states carries more information than a pair of identical coherent states [20]. These results enable one to achieve better fidelities with a cloning

*Corresponding author. jzhang74@yahoo.com; jzhang74@sxu.edu.cn

TABLE I. Summary of earlier work and existing results on quantum cloning.

Local cloning	Conventional cloning with identical inputs	Discrete variables	Bužek and Hillery [5]; Lamas-Linares *et al.* (experiment) [31]; De Martini*et al.* (experiment) [31]
		Continuous variables	Cerf *et al.* (theory) [6]; D'Ariano *et al.* (theory) [7]; Braunstein *et al.* (theory) [8]; Andersen *et al.* (experiment, irreversible) [23]
	Local cloning with (antiparallel) phase-conjugate inputs	Discrete variables	Fiurášek (theory) [21]
		Continuous variables	Cerf and Iblisdir (theory, reversible) [22]; Chen and Zhang (theory, irreversible and reversible) [23]; Sabuncu *et al.* (experiment, irreversible) [24]
Nonlocal cloning	Conventional nonlocal cloning (telecloning) with identical inputs	Discrete variables	Bruβ *et al.* (theory, irreversible) [16]; Dür (theory, irreversible) [16]; Murao *et al.* (theory, reversible) [16]; Zhao *et al.* (experiment) [32]
		Continuous variables	van Loock and Braunstein (theory, irreversible) [12]; Zhang *et al.* (theory, reversible) [18]; Koike *et al.* (experiment, irreversible) [17]
	Nonlocal cloning (telecloning) with (antiparallel) phase-conjugate inputs	Discrete variables	
		Continuous variables	Current work

machine admitting antiparallel input qubits or phase-conjugate input coherent states, compared to the conventional case with identical input copies. Based upon the above properties, Fiurášek *et al.* proposed a cloning machine for antiparallel spin states [21]. Similarly, Cerf and Iblisdir derived a CV cloning transformation [22] that uses N copies of a coherent state and N' copies of its complex conjugate as input states, and produces M optimal clones of the coherent state and $M'=M+N'-N$ phase-conjugate clones (anticlones, or time-reversed states). This is the first scheme for a local, phase-conjugate input (PCI) cloner of continuous variables. Nonetheless, an experimental realization of the proposed PCI cloner is difficult, as it requires "online" optical parametric amplification. Recently, a much simpler and efficient CV PCI cloning machine based on linear optics, homodyne detection, and feedforward was proposed [23,24] and implemented experimentally [24]. Note that the production of an infinite number of clones ($M\rightarrow\infty$) coincides with optimal or perfect state estimation [25]. The case of M clones and $M-2$ anticlones from two identical replicas gives the optimal telecloning fidelity of 2/3 for $M\rightarrow\infty$ and the maximally Einstein-Podolsky-Rosen (EPR) entangled state. This is consistent with the standard optimal value of 2/3 for $1\rightarrow 2$ cloning of coherent states that was obtained in Ref. [6]. However, the PCI telecloner yields the better fidelity of 4/5 owing to the added information in the phase-conjugate input state. The result of the increased fidelity of 4/5 for coherent states with phase-conjugate input modes indicates that the added information in the input state must be equivalent to the $1\rightarrow 2$ cloning of a single-mode coherent state with known phase, where the fidelity is also 4/5 [26]. A summary of the various quantum cloning schemes and their realizations is shown in Table I.

In this paper, we propose a protocol of CV reversible telecloning of coherent states with phase-conjugate input modes. The $N+N\rightarrow M+M$ quantum telecloning machine yields M identical clones and M identical anticlones from N copies of a coherent state and N phase-conjugate copies. Here, we consider two cases of PCI telecloning. In the first case, PCI telecloning produces M clones nonlocally and M anticlones locally, or vice versa. Alternatively, both clones and anticlones may be created nonlocally through PCI telecloning. Optimal cloning fidelities of this PCI telecloning require perfect EPR entanglement, i.e., infinite two-mode squeezing as a resource. However, similar to the conventional (irreversible) CV telecloning scheme [12], no "online" optical parametric amplification is needed. As shown in Table I, PCI telecloning of qubit states has not been investigated yet. Hence our protocol represents a nice example, where a CV quantum information protocol is proposed before its qubit counterpart.

II. PCI TELECLONING WITH NONLOCAL CLONES AND LOCAL ANTICLONES, $1+1\rightarrow M+M$

The quantum states we consider in this paper are described with the electromagnetic field annihilation operator $\hat{a}=(\hat{X}+i\hat{P})/2$, which is expressed in terms of the amplitude $\hat{X}$ and phase $\hat{P}$ quadrature with the canonical commutation relation $[\hat{X},\hat{P}]=2i$. Without loss of generality, the quadrature operators can be expressed in terms of a steady state and fluctuating component as $\hat{A}=\langle\hat{A}\rangle+\Delta\hat{A}$, with variances of $V_A=\langle\Delta\hat{A}^2\rangle$ ($\hat{A}=\hat{X}$ or $\hat{P}$). The input coherent state and its phase-conjugate state to be cloned will be described by $|\alpha_{\text{in}}\rangle=|\frac{1}{2}(x_{\text{in}}+ip_{\text{in}})\rangle$ and $|\alpha_{\text{in}}^{*}\rangle=|\frac{1}{2}(x_{\text{in}}-ip_{\text{in}})\rangle$, respectively, where x_{in} and p_{in} are the expectation values of $\hat{X}_{\text{in}}$ and $\hat{P}_{\text{in}}$. The cloning machine generates many clones of the input state characterized by the density operator $\hat{\rho}_{\text{clone}}$ and the expecta-

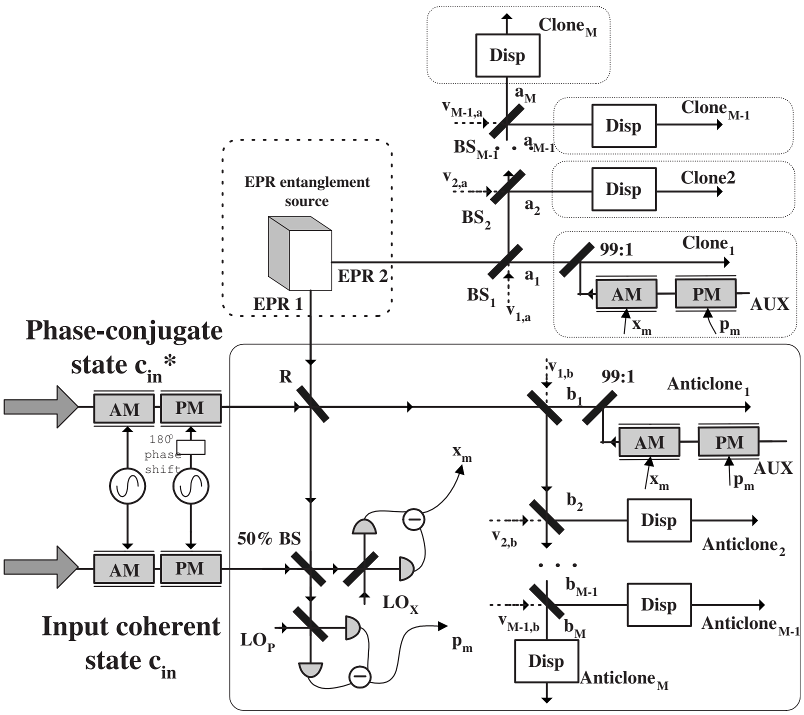

FIG. 1. Schematic diagram of $1+1 \rightarrow M+M$ PCI telecloning with nonlocal clones and local anticlones. BS, beam splitter; LO, local oscillator; AM, amplitude modulator; PM, phase modulator; and AUX, auxiliary beam.

tion values x_{clone} and p_{clone}. The quality of the cloning machine can be quantified by the fidelity, which is the overlap between the input state and the output state. It is defined by [27]

$$F = \langle \alpha_{\text{in}} | \hat{\rho}_{\text{clone}} | \alpha_{\text{in}} \rangle = \frac{2}{\sqrt{(1+\Delta^2 \hat{X}_{\text{clone}})(1+\Delta^2 \hat{P}_{\text{clone}})}} \times \exp\left(- \frac{(x_{\text{clone}} - x_{\text{in}})^2}{2(1+\Delta^2 \hat{X}_{\text{clone}})} - \frac{(p_{\text{clone}} - p_{\text{in}})^2}{2(1+\Delta^2 \hat{P}_{\text{clone}})} \right). \tag{1}$$

In the case of unity gains, i.e., $x_{\text{clone}} = x_{\text{in}}$, the fidelity is strongly peaked and becomes

$$F = \frac{2}{\sqrt{(1+\Delta^2 \hat{X}_{\text{clone}})(1+\Delta^2 \hat{P}_{\text{clone}})}}. \tag{2}$$

The essence of quantum telecloning is the multipartite entanglement shared among the sender and the receivers. Without multipartite entanglement, it is only possible to perform the corresponding two-step protocol: The sender produces clones and anticlones locally, and then (bipartitely) teleports them to each receiver. The two-step protocol would require $2M-1$ bipartite entanglement for teleportation. Continuous-variable PCI telecloning with nonlocal clones and local anticlones only requires one resource of bipartite entanglement. The bipartite entangled state of CV is a two-mode Gaussian entangled state (EPR entangled state), which can be obtained directly by type-II parametric interaction [28] or indirectly by mixing two independent squeezed beams on a beam splitter [27]. The EPR entangled beams have a very strong correlation property such that both their sum-amplitude quadrature variance $\langle \delta(\hat{X}_{a_{\text{EPR1}}} + \hat{X}_{a_{\text{EPR2}}})^2 \rangle = 2e^{-2r}$ and their difference-phase quadrature variance $\langle \delta(\hat{P}_{a_{\text{EPR1}}} - \hat{P}_{a_{\text{EPR2}}})^2 \rangle = 2e^{-2r}$ are below the two-mode vacuum noise limit, where r is the squeezing parameter. Let us first illustrate the protocol in the simple case of $1+1 \rightarrow M+M$ PCI telecloning, as shown in Fig. 1. One of the EPR entangled beams $\hat{a}_{\text{EPR1}}$ is held by the sender and the other $\hat{a}_{\text{EPR2}}$ is distributed among M remote parties via $(M-1)$ beam splitters with appropriately adjusted transmittances and reflectivity's. The modes $\hat{v}_{j,a}$ are in the vacuum state. The EPR entangled mode $\hat{a}_{\text{EPR2}}$ is mixed with $\hat{v}_{1,\text{in}}$ at the beam splitter BS$_1$. The mode $\hat{a}_1$ contains the EPR entangled mode $\hat{a}_{\text{EPR2}}$ up to a factor of $1/\sqrt{M}$. The output $\hat{c}_2$ is split at BS$_2$ and so on, until it arrives at the last beam splitter BS$_{M-1}$. The transformation performed by the jth beam splitter can be written as

$$\hat{a}_j = \sqrt{\frac{1}{M-j+1}} \hat{c}_{j,a} + \sqrt{\frac{M-j}{M-j+1}} \hat{v}_{j,a},$$

$$\hat{c}_{j+1,a} = \sqrt{\frac{M-j}{M-j+1}} \hat{c}_{j,a} - \sqrt{\frac{1}{M-j+1}} \hat{v}_{j,a}, \tag{3}$$

where $\hat{c}_{1,a} = \hat{a}_{\text{EPR2}}$ and $\hat{a}_M = \hat{c}_{M,a}$. It is clearly shown that each mode $\hat{a}_j$ contains a $\sqrt{1/M}$ portion of the EPR entangled mode $\hat{a}_{\text{EPR2}}$ and a $\sqrt{(M-1)/M}$ portion of vacuum.

At the sender station, the input coherent state $\hat{c}_{\text{in}}$ and its phase-conjugate state $\hat{c}_{\text{in}}^*$ are prepared by an amplitude modulator and a phase modulator, respectively. The modulated signals on the amplitude modulators are in phase and the modulated signals on the phase modulators are out of phase. The input phase-conjugate state $\hat{c}_{\text{in}}^*$ is combined with the EPR entangled beam $\hat{a}_{\text{EPR1}}$ via a variable beam splitter BS$_0$ with transmission rate T and reflectivity rate R. The transmitted field $\hat{c}_{1t} = \sqrt{T} \hat{c}_{\text{in}}^* - \sqrt{R} \hat{a}_{\text{EPR1}}$ is divided into M modes $\{\hat{b}_1, \hat{b}_2, \ldots, \hat{b}_M\}$ via $(M-1)$ beam splitters, which is the same as for the EPR entangled beam $\hat{a}_{\text{EPR2}}$ [see also Eq.

(3)]. The reflected output $\hat{c}_{1r}=\sqrt{R}\hat{c}_{\text{in}}^{*}+\sqrt{T}\hat{a}_{\text{EPR1}}$ is combined with input mode $\hat{c}_{\text{in}}$ at a 50/50 beam splitter. Then we perform homodyne measurements on the two output beams in order to obtain the amplitude and phase quadratures simultaneously. The measured quadratures are

$$\hat{X}_m=\frac{1}{\sqrt{2}}(\sqrt{R}\hat{X}_{c_{\text{in}}^{*}}+\sqrt{T}\hat{X}_{\text{EPR1}}+\hat{X}_{c_{\text{in}}}),$$

$$\hat{P}_m=\frac{1}{\sqrt{2}}(\sqrt{R}\hat{P}_{c_{\text{in}}^{*}}+\sqrt{T}\hat{P}_{\text{EPR1}}-\hat{P}_{c_{\text{in}}}). \tag{4}$$

The sender then conveys the measured results x_m and p_m to the local modes $\hat{b}_j$ and the remote ones $\hat{a}_j$. After receiving the measurement results, each receiver displaces his corresponding mode by means of a 1/99 beam splitter with an auxiliary beam, the amplitude and phase of which have been modulated via two independent modulators using the received x and p signals with the scaling factors $g_x=-g_p=g_1$ for modes $\hat{a}_j$, and $g_x=g_p=g_2$ for modes $\hat{b}_j$, respectively [24]. Corresponding to the transformation $\hat{A}\rightarrow\hat{D}^{\dagger}\hat{A}\hat{D}=\hat{A}+(\hat{X}_m+i\hat{P}_m)/2$ in the Heisenberg representation, the displaced fields of the remote parties can be expressed as

$$\hat{a}_j'=\sqrt{\frac{1}{M-j+1}}\hat{c}_{j,a}'+\sqrt{\frac{M-j}{M-j+1}}\hat{v}_{j,a},$$

$$\hat{c}_{j+1,a}'=\sqrt{\frac{M-j}{M-j+1}}\hat{c}_{j,a}'-\sqrt{\frac{1}{M-j+1}}\hat{v}_{j,a}, \tag{5}$$

where

$$\hat{c}_{1,a}'=g_1\sqrt{\frac{M}{2}}\sqrt{R}\hat{c}_{\text{in}}^{*\dagger}+g_1\sqrt{\frac{M}{2}}\sqrt{1-R}\hat{a}_{\text{EPR1}}^{\dagger}+\hat{a}_{\text{EPR2}}+g_1\sqrt{\frac{M}{2}}\hat{c}_{\text{in}}, \tag{6}$$

$$\hat{a}_M'=\hat{c}_{M,a}'. \tag{7}$$

The displaced local modes can be expressed as

$$\hat{b}_j'=\sqrt{\frac{1}{M-j+1}}\hat{c}_{j,b}'+\sqrt{\frac{M-j}{M-j+1}}\hat{v}_{j,b},$$

$$\hat{c}_{j+1,b}'=\sqrt{\frac{M-j}{M-j+1}}\hat{c}_{j,b}'-\sqrt{\frac{1}{M-j+1}}\hat{v}_{j,b}, \tag{8}$$

where

$$\hat{c}_{1,b}'=\left(\sqrt{1-R}+g_2\sqrt{\frac{M}{2}}\sqrt{R}\right)\hat{c}_{\text{in}}^{*}-\left(\sqrt{R}-g_2\sqrt{\frac{M}{2}}\sqrt{1-R}\right)\hat{a}_{\text{EPR1}}+g_2\sqrt{\frac{M}{2}}\hat{c}_{\text{in}}^{\dagger}, \tag{9}$$

$$\hat{b}_M'=\hat{c}_{M,b}'. \tag{10}$$

By choosing $g_1=\sqrt{2/M(1-R)}$ and $g_2=\sqrt{2R/M(1-R)}$, the displaced fields $\hat{c}_{1,a}'$ and $\hat{c}_{1,b}'$ are given by

$$\hat{c}_{1,a}'=\frac{\sqrt{R}}{\sqrt{1-R}}\hat{c}_{\text{in}}^{*\dagger}+\frac{1}{\sqrt{1-R}}\hat{c}_{\text{in}}+(\hat{a}_{\text{EPR1}}^{\dagger}+\hat{a}_{\text{EPR2}}), \tag{11}$$

$$\hat{c}_{1,b}'=\frac{1}{\sqrt{1-R}}\hat{c}_{\text{in}}^{*}+\frac{\sqrt{R}}{\sqrt{1-R}}\hat{c}_{\text{in}}^{\dagger}. \tag{12}$$

We can see that Eqs. (11) and (12) include a phase-insensitive amplification with gain $G=1/(1-R)$.

Note that both terms $\hat{c}_{\text{in}}$ and $\hat{c}_{\text{in}}^{*\dagger}$ in Eq. (11) contribute to the total coherent signal with a factor of $1/\sqrt{1-R}+\sqrt{R}/\sqrt{1-R}$ and noise variances with $\sqrt{1+R}/\sqrt{1-R}$, and in Eq. (12) they contribute to the total conjugate coherent signal with a factor of $1/\sqrt{1-R}+\sqrt{R}/\sqrt{1-R}$ and noise variances with $\sqrt{1+R}/\sqrt{1-R}$. Since each output cloner $\hat{a}_j'$ and anticlone $\hat{b}_j'$ should include one part of the input coherent and the conjugate state, R must satisfy

$$\frac{1}{\sqrt{M(1-R)}}+\frac{\sqrt{R}}{\sqrt{M(1-R)}}=1. \tag{13}$$

The parameter R can be easily determined by solving the above equation,

$$R=\frac{(M-1)^2}{(M+1)^2}. \tag{14}$$

According to Eqs. (5), (8), and (14), the variances of the clones and anticlones can be written as

$$\Delta^2\hat{X}_{a_j'}=\Delta^2\hat{P}_{a_j'}=1+\frac{(M-1)^2}{2M^2}+\frac{2e^{-2r}}{M},$$

$$\Delta^2\hat{X}_{b_j'}=\Delta^2\hat{P}_{b_j'}=\frac{1}{M}\frac{1+R}{1-R}+\frac{M-1}{M}=1+\frac{(M-1)^2}{2M^2}. \tag{15}$$

The fidelity can be obtained via Eq. (2),

$$F^{\text{clone}}_{\binom{1}{1}\rightarrow\binom{M}{M}}=\frac{4M^2}{4M^2+(M-1)^2+4Me^{-2r}},$$

$$F^{\text{anti}}_{\binom{1}{1}\rightarrow\binom{M}{M}}=\frac{4M^2}{4M^2+(M-1)^2}. \tag{16}$$

This scheme produces M anticlones locally and M clones nonlocally. The fidelity of the anticlones is optimal and independent of the entanglement. However, the fidelity of the clones does depend on the entanglement. An optimal fidelity of the clones requires a maximally EPR entangled state, $r\rightarrow\infty$. Now we compare M clones and M anticlones from the phase-conjugate input modes with M clones and $M-2$ anticlones from the two identical replicas. The fidelity of the standard 2-to-$M+(M-2)$ telecloning is given by [18]

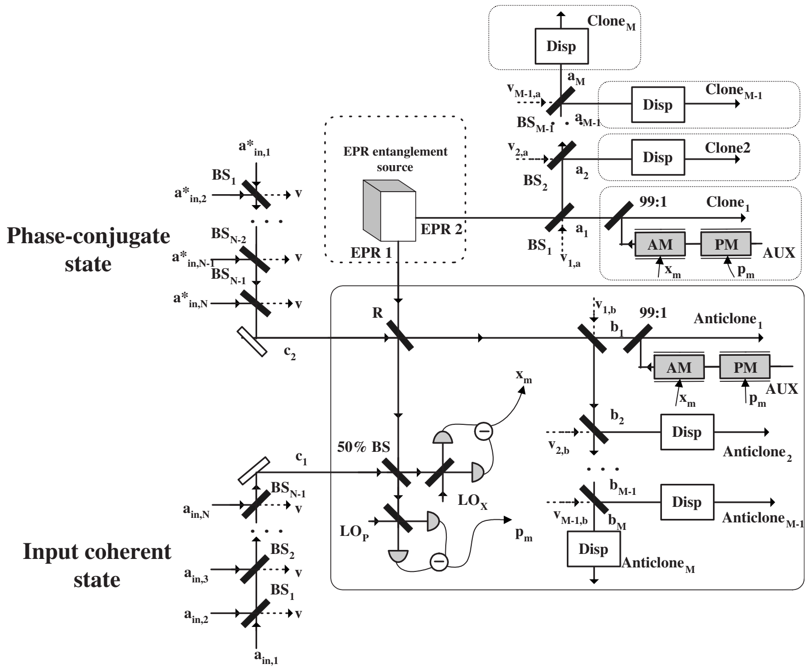

FIG. 2. Schematic diagram of $N+N\rightarrow M+M$ PCI telecloning with nonlocal clones and local anticlones.

$$F^{\text{clone}}_{2\rightarrow M+(M-2)} = \frac{2M}{3M-2+2e^{-2r}}, \tag{17}$$

$$F^{\text{anti}}_{2\rightarrow M+(M-2)} = \frac{2}{3}. \tag{18}$$

In the special case $M=2$, the standard telecloner can produce clones perfectly with fidelity equal to 1 ($r\rightarrow\infty$) and no anticlones, while the PCI telecloner yields two clones and two anticlones with fidelity equal to 16/17 ($r\rightarrow\infty$). Obviously, the PCI telecloner yields a better fidelity than the standard cloning when $M\geq 3$. In the limit of large $M\rightarrow\infty$, we see $F^{\text{clone}}_{\binom{1}{1}\rightarrow\infty}=F^{\text{anti}}_{\binom{1}{1}\rightarrow\infty}=\frac{4}{5}$ compared with the standard telecloning $F^{\text{clone}}_{2\rightarrow\infty}=F^{\text{anti}}_{2\rightarrow\infty}=\frac{2}{3}$ ($r\rightarrow\infty$). This shows that more information can be encoded into a pair of conjugate coherent states than by using two identical states, which was shown in Refs. [20,24]. This scheme can be easily modified in order to realize PCI telecloning with local clones and nonlocal anticlones; simply the inputs of the coherent state and its phase-conjugate state must be swapped.

III. PCI TELECLONING WITH NONLOCAL CLONES AND LOCAL ANTICLONES, $N+N\rightarrow M+M$

We now generalize the $1+1\rightarrow M+M$ case to $N+N\rightarrow M+M$ PCI quantum telecloning, which produces M clones nonlocally and M anticlones locally from N copies of a coherent state and N copies of its complex conjugate, as illustrated in Fig. 2. First, we concentrate N identically prepared coherent states $|\Phi\rangle$ described by $\{\hat{a}_{\text{in},l}\}$ ($l=1,\ldots,N$) into a single spatial mode $\hat{c}_1$ with amplitude $\sqrt{N}\Phi$. This operation can be performed by interfering N input modes in $N-1$ beam splitters, which yields the mode

$$\hat{c}_1 = \frac{1}{\sqrt{N}}\sum_{l=1}^{N}\hat{a}_{\text{in},l} \tag{19}$$

and $N-1$ vacuum modes. The same method can be used for the generation of the phase-conjugate input mode $\hat{c}_2$ with amplitude $\sqrt{N}\Phi^*$ from the N copies of $|\Phi^*\rangle$ stored in the N modes $\{a^*_{\text{in},l}\}$ ($l=1,\ldots,N$), which is expressed as

$$\hat{c}_2 = \frac{1}{\sqrt{N}}\sum_{l=1}^{N}\hat{a}^*_{\text{in},l}. \tag{20}$$

Then, $\hat{c}_1$ and $\hat{c}_2$ are sent into the cloning machine (see Fig. 1). The displaced fields [Eqs. (11) and (12)] become

$$\hat{c}'_{1,a} = \frac{\sqrt{R}}{\sqrt{1-R}}\hat{c}_2^\dagger + \frac{1}{\sqrt{1-R}}\hat{c}_1 + (\hat{a}^\dagger_{\text{EPR1}} + \hat{a}_{\text{EPR2}}), \tag{21}$$

$$\hat{c}'_{1,b} = \frac{1}{\sqrt{1-R}}\hat{c}_2 + \frac{\sqrt{R}}{\sqrt{1-R}}\hat{c}_1^\dagger. \tag{22}$$

The terms with $\hat{c}_1$ and $\hat{c}_2^\dagger$ in Eqs. (21) and (22) contribute to the total coherent signal with a factor of $\sqrt{N}(1/\sqrt{1-R}+\sqrt{R}/\sqrt{1-R})$ and noise variances with $\sqrt{(1+R)/(1-R)}$. Since each output cloner $\hat{a}'_j$ and anticlone $\hat{b}'_j$ should again include one part of the input coherent and conjugate state, R must satisfy

$$\sqrt{N}\left(\frac{1}{\sqrt{M(1-R)}} + \frac{\sqrt{R}}{\sqrt{M(1-R)}}\right) = 1. \tag{23}$$

The parameter R can be easily determined by solving the above equation,

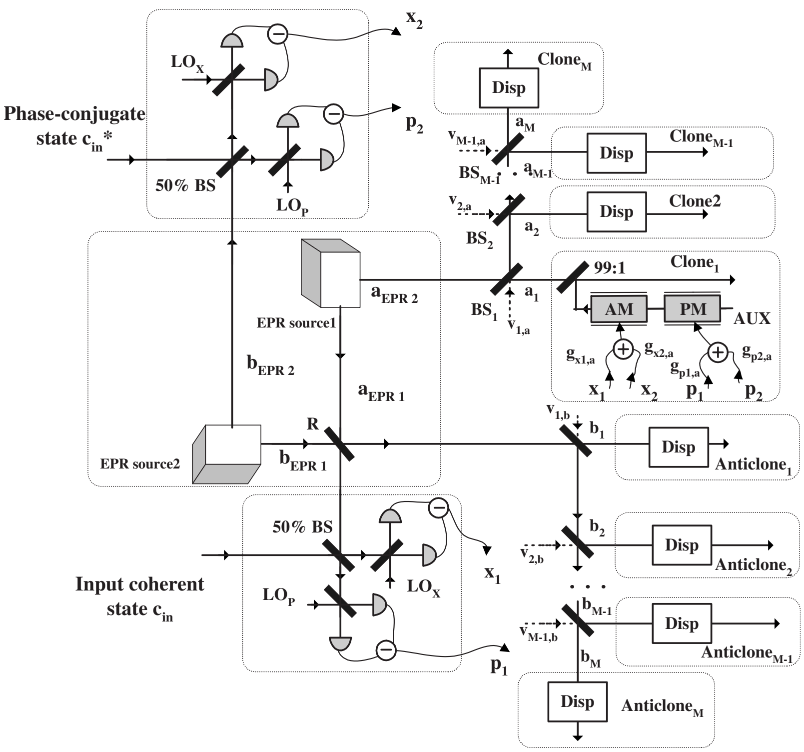

FIG. 3. Schematic diagram of $1+1\rightarrow M+M$ PCI telecloning with both clones and anticlones nonlocal.

$$R=\frac{(M-N)^2}{(M+N)^2}. \tag{24}$$

The variance and fidelity of the $\binom{N}{N}\rightarrow\binom{M}{M}$ PCI telecloner is now given by

$$\Delta^2\hat{X}_{a_j'}=\Delta^2\hat{P}_{a_j'}=1+\frac{(M-N)^2}{2M^2N}+\frac{2e^{-2r}}{M},$$

$$\Delta^2\hat{X}_{b_j'}=\Delta^2\hat{P}_{b_j'}=1+\frac{(M-N)^2}{2M^2N},$$

$$F^{\text{clone}}_{\binom{N}{N}\rightarrow\binom{M}{M}}=\frac{4M^2N}{4M^2N+(M-N)^2+4MNe^{-2r}},$$

$$F^{\text{anti}}_{\binom{N}{N}\rightarrow\binom{M}{M}}=\frac{4M^2N}{4M^2N+(M-N)^2}. \tag{25}$$

Obviously, Eq. (16) can be obtained from Eq. (25) with $N=1$. This result also coincides with that obtained in Refs. [22,29]. However, the output anticlones are lost in that scheme. The advantage of dealing with N pairs of complex conjugate inputs can be most easily illustrated in the limit of an infinite number of clones, $M\rightarrow\infty$; from Eq. (25) we obtain $F^{\text{clone}}_{\binom{N}{N}\rightarrow\binom{M}{M}}=\frac{4N}{4N+1}$ and $F^{\text{anti}}_{\binom{N}{N}\rightarrow\binom{M}{M}}=\frac{4N}{4N+1}$, while the standard telecloning fidelities are $F^{\text{clone}}_{2N\rightarrow M+(M-2N)}=\frac{2N}{2N+1}$ and $F^{\text{anti}}_{2N\rightarrow M+(M-2N)}=\frac{2N}{2N+1}$ $(r\rightarrow\infty)$.

IV. PCI TELECLONING WITH BOTH CLONES AND ANTICLONES NONLOCAL

We now consider $1+1\rightarrow M+M$ PCI telecloning, which nonlocally produces at the same time M clones and M anticlones from a coherent state and its phase conjugate using multipartite entanglement, as shown in Fig. 3. The case of $N+N\rightarrow M+M$ is easily obtained from the case of $1+1\rightarrow M+M$ in a similar way to the discussion of the preceding sections.

Here, two pairs $(\hat{a}_{\text{EPR1}},\hat{a}_{\text{EPR2}})$ and $(\hat{b}_{\text{EPR1}},\hat{b}_{\text{EPR2}})$ of EPR entanglement are utilized with squeezing r_1 and r_2, respectively. One of the EPR entangled beams $\hat{a}_{\text{EPR2}}$ is distributed among M remote parties $\{\hat{a}_1,\hat{a}_2,\ldots,\hat{a}_M\}$ via $(M-1)$ beam splitters similar to Eq. (3). One of the other EPR entangled beams $\hat{b}_{\text{EPR1}}$ is combined with the EPR entangled beam $\hat{a}_{\text{EPR1}}$ at a beam splitter BS_0 with transmission rate $T=1-R$ and reflectivity $R=(M-1)^2/(M+1)^2$. The transmitted field $\hat{c}_{1t}=\sqrt{T}\hat{b}_{\text{EPR1}}-\sqrt{R}\hat{a}_{\text{EPR1}}$ is also divided into M remote modes $\{\hat{b}_1,\hat{b}_2,\ldots,\hat{b}_M\}$ by $(M-1)$ beam splitters, similar to the EPR entangled beam $\hat{a}_{\text{EPR2}}$. The reflected output $\hat{c}_{1r}=\sqrt{R}\hat{b}_{\text{EPR1}}+\sqrt{T}\hat{a}_{\text{EPR1}}$ and $\hat{b}_{\text{EPR2}}$ are held by the senders 1 and 2, respectively. Sender 1 combines the reflected output mode $\hat{c}_{1r}$ with input mode $\hat{c}_{\text{in}}$ at a 50/50 beam splitter and sender 2 does the same thing with the EPR entangled beam $\hat{b}_{\text{EPR2}}$ and the phase-conjugate input mode. Note that the modes $\hat{a}_{\text{EPR2}}$, $\hat{c}_{1t}$, $\hat{c}_{1r}$, and $\hat{b}_{\text{EPR2}}$ form a genuine four-mode entangled state, whose properties are different from CV Greenberger-Horne-Zeilinger and cluster states discussed in Ref. [30]. Next the senders perform homodyne measurements on the two output beams of the 50/50 beam splitters to obtain two amplitude and phase-quadrature measurement results (x_1,p_1), (x_2,p_2) to be conveyed to the remote parties. The measured quadratures are

$$\hat{X}_1 = \frac{1}{\sqrt{2}}(\sqrt{R}\hat{X}_{b_{\mathrm{EPR1}}} + \sqrt{T}\hat{X}_{a_{\mathrm{EPR1}}} + \hat{X}_{c_{\mathrm{in}}}),$$

$$\hat{P}_1 = \frac{1}{\sqrt{2}}(\sqrt{R}\hat{P}_{b_{\mathrm{EPR1}}} + \sqrt{T}\hat{P}_{a_{\mathrm{EPR1}}} - \hat{P}_{c_{\mathrm{in}}}),$$

$$\hat{X}_2 = \frac{1}{\sqrt{2}}(\hat{X}_{b_{\mathrm{EPR2}}} + \hat{X}_{c^*_{\mathrm{in}}}),$$

$$\hat{P}_2 = \frac{1}{\sqrt{2}}(\hat{P}_{b_{\mathrm{EPR2}}} - \hat{P}_{c^*_{\mathrm{in}}}). \tag{26}$$

After receiving the measurement results, each party in the set $\{\hat{a}_1, \hat{a}_2, \ldots, \hat{a}_M\}$ combines these results,

$$x_{s,a} = g_{x1,a}x_1 + g_{x2,a}x_2 = \frac{1}{\sqrt{M}}\left(\sqrt{\frac{R}{1-R}}\hat{X}_{c^*_{\mathrm{in}}} + \hat{X}_{a_{\mathrm{EPR1}}} + \sqrt{\frac{1}{1-R}}\hat{X}_{c_{\mathrm{in}}}\right) + \sqrt{\frac{R}{M(1-R)}}(\hat{X}_{b_{\mathrm{EPR1}}} + \hat{X}_{b_{\mathrm{EPR2}}}),$$

$$p_{s,a} = g_{p1,a}p_1 + g_{p2,a}p_2 = -\frac{1}{\sqrt{M}}\left(\sqrt{\frac{R}{1-R}}\hat{P}_{c^*_{\mathrm{in}}} + \hat{P}_{a_{\mathrm{EPR1}}} - \sqrt{\frac{1}{1-R}}\hat{P}_{c_{\mathrm{in}}}\right) + \sqrt{\frac{R}{M(1-R)}}(\hat{P}_{b_{\mathrm{EPR2}}} - \hat{P}_{b_{\mathrm{EPR1}}}), \tag{27}$$

where $g_{x1,a}=-g_{p1,a}=g_{x2,a}/\sqrt{R}=-g_{p2,a}/\sqrt{R}=\sqrt{2/M(1-R)}$, and finally displaces the corresponding entangled mode. The output fields are the clones of PCI telecloning with the variances and fidelity given by

$$\Delta^2\hat{X}_{a'_j} = \Delta^2\hat{P}_{a'_j} = 1 + \frac{(M-1)^2}{2M^2}(1+e^{-2r_2}) + \frac{2e^{-2r_1}}{M},$$

$$F^{\mathrm{clone}}_{\binom{1}{1}\to\binom{M}{M}} = \frac{4M^2}{4M^2 + (M-1)^2(1+e^{-2r_2}) + 4Me^{-2r_1}}. \tag{28}$$

Similarly, each party in the set $\{\hat{b}_1, \hat{b}_2, \ldots, \hat{b}_M\}$ combines the measurement results,

$$x_{s,b} = g_{x1,b}x_1 + g_{x2,b}x_2 = \frac{1}{\sqrt{M}}\left(\sqrt{\frac{1}{1-R}}\hat{X}_{c^*_{\mathrm{in}}} + \sqrt{R}\hat{X}_{a_{\mathrm{EPR1}}} + \sqrt{\frac{R}{1-R}}\hat{X}_{c_{\mathrm{in}}} + \frac{1}{\sqrt{1-R}}\hat{X}_{b_{\mathrm{EPR2}}}\right) + \frac{R}{\sqrt{M(1-R)}}\hat{X}_{b_{\mathrm{EPR1}}},$$

$$p_{s,b} = g_{p1,b}p_1 + g_{p2,b}p_2 = \frac{1}{\sqrt{M}}\left(\sqrt{\frac{1}{1-R}}\hat{P}_{c^*_{\mathrm{in}}} + \sqrt{R}\hat{P}_{a_{\mathrm{EPR1}}} - \sqrt{\frac{R}{1-R}}\hat{P}_{c_{\mathrm{in}}} - \frac{1}{\sqrt{1-R}}\hat{P}_{b_{\mathrm{EPR2}}}\right) + \frac{R}{\sqrt{M(1-R)}}\hat{P}_{b_{\mathrm{EPR1}}}, \tag{29}$$

where $g_{x1,b}=g_{p1,b}=\sqrt{2R/M(1-R)}$ and $g_{x2,b}=-g_{p2,b}=\sqrt{2/M(1-R)}$, and finally displaces the corresponding entangled mode. Now the output fields are the anticlones of PCI telecloning with the variances and fidelity

$$\Delta^2\hat{X}_{b'_j} = \Delta^2\hat{P}_{b'_j} = 1 + \frac{(M-1)^2}{2M^2} + \frac{(M+1)^2}{2M^2}e^{-2r_2},$$

$$F^{\mathrm{anti}}_{\binom{1}{1}\to\binom{M}{M}} = \frac{4M^2}{4M^2 + (M-1)^2 + (M+1)^2 e^{-2r_2}}. \tag{30}$$

This protocol produces nonlocally M clones and M anticlones at the same time. The fidelity of the clones and anticlones depends on the entanglement. Clearly, an optimal fidelity of the clones and anticlones, in agreement with the results of Refs. [22,29], requires a perfectly entangled state, r_1, $r_2 \to \infty$.

V. CONCLUSION

In conclusion, we have proposed a protocol for CV telecloning of coherent states with phase-conjugate input modes. Two kinds of PCI telecloning are considered. In the first scheme, the PCI telecloning produces clones nonlocally and anticlones locally. Realization of this kind of PCI telecloning requires a single EPR (two-mode squeezed) entangled state as a resource, arrays of beam splitters, homodyne detection, and feedforward. Through the alternative scheme, both clones and anticlones are produced nonlocally at the same time. This scheme requires two EPR entangled states as a resource. The protocols described here may be applicable to various quantum communication scenarios, e.g., to an eavesdropping attack in quantum key distribution.

ACKNOWLEDGMENTS

This research was supported in part by NSFC for Distinguished Young Scholars (Grant No. 10725416), National Basic Research Proram of China (Grant No. 2006CB921101), NSFC (Grants No. 60678029 and No. 60736040), Doctoral Program Foundation of Ministry of Education China (Grant No. 20050108007), Program for Changjiang Scholars and Innovative Research Team in University, Natural Science Foundation of Shanxi Province (Grant No. 2006011003), and the Research Fund for the Returned Abroad Scholars of Shanxi Province. One of the authors (P.vL.) acknowledges funding from the DFG under the Emmy Noether program.

[1] W. K. Wootters and W. H. Zurek, Nature (London) **299**, 802 (1982).
[2] D. Dieks, Phys. Lett. **92A**, 271 (1982).
[3] E. F. Galvao and L. Hardy, Phys. Rev. A **62**, 022301 (2000).
[4] N. Gisin, G. G. Ribordy, W. Tittel, and H. Zbinden, Rev. Mod. Phys. **74**, 145 (2002).
[5] V. Bužek and M. Hillery, Phys. Rev. A **54**, 1844 (1996).
[6] N. J. Cerf, A. Ipe, and X. Rottenberg, Phys. Rev. Lett. **85**, 1754 (2000).
[7] G. M. D'Ariano, F. De Martini, and M. F. Sacchi, Phys. Rev. Lett. **86**, 914 (2001).
[8] S. L. Braunstein, N. J. Cerf, S. Iblisdir, P. van Loock, and S. Massar, Phys. Rev. Lett. **86**, 4938 (2001).
[9] J. Fiurášek, Phys. Rev. Lett. **86**, 4942 (2001).
[10] V. Josse, M. Sabuncu, N. J. Cerf, G. Leuchs, and U. L. Andersen, Phys. Rev. Lett. **96**, 163602 (2006).
[11] J. Fiurášek, N. J. Cerf, and E. S. Polzik, Phys. Rev. Lett. **93**, 180501 (2004).
[12] P. van Loock and S. L. Braunstein, Phys. Rev. Lett. **87**, 247901 (2001).
[13] S. L. Braunstein and H. J. Kimble, Phys. Rev. Lett. **80**, 869 (1998).
[14] A. Ferraro and M. G. A. Paris, Phys. Rev. A **72**, 032312 (2005).
[15] G. Adesso, A. Serafini, and F. Illuminati, New J. Phys. **9**, 60 (2007).
[16] D. Bruβ, D. P. DiVincenzo, A. Ekert, C. A. Fuchs, C. Macchiavello, and J. A. Smolin, Phys. Rev. A **57**, 2368 (1998); W. Dür, *ibid.* **63**, 020303(R) (2001); M. Murao, D. Jonathan, M. B. Plenio, and V. Vedral, Phys. Rev. A **59**, 156 (1999).
[17] S. Koike, H. Takahashi, H. Yonezawa, N. Takei, S. L. Braunstein, T. Aoki, and A. Furusawa, Phys. Rev. Lett. **96**, 060504 (2006).
[18] J. Zhang, C. Xie, and K. Peng, Phys. Rev. A **73**, 042315 (2006).
[19] N. Gisin and S. Popescu, Phys. Rev. Lett. **83**, 432 (1999).
[20] N. J. Cerf and S. Iblisdir, Phys. Rev. A **64**, 032307 (2001).
[21] J. Fiurášek, S. Iblisdir, S. Massar, and N. J. Cerf, Phys. Rev. A **65**, 040302(R) (2002).
[22] N. J. Cerf and S. Iblisdir, Phys. Rev. Lett. **87**, 247903 (2001).
[23] H. Chen and J. Zhang, Phys. Rev. A **75**, 022306 (2007).
[24] M. Sabuncu, U. L. Andersen, and G. Leuchs, Phys. Rev. Lett. **98**, 170503 (2007).
[25] J. Bae and A. Acin, Phys. Rev. Lett. **97**, 030402 (2006).
[26] M. Alexanian, Phys. Rev. A **73**, 045801 (2006).
[27] A. Furusawa *et al.*, Science **282**, 706 (1998).
[28] Z. Y. Ou, S. F. Pereira, H. J. Kimble, and K. C. Peng, Phys. Rev. Lett. **68**, 3663 (1992); Y. Zhang, H. Wang, X. Li, J. Jing, C. Xie, and K. Peng, Phys. Rev. A **62**, 023813 (2000).
[29] N. J. Cerf and S. Iblisdir, Phys. Rev. A **62**, 040301(R) (2000).
[30] J. Zhang, C. Xie, and K. Peng, Phys. Rev. A **76**, 064301 (2007).
[31] A. Lamas-Linares, C. Simon, J. C. Howell, and D. Bouwmeester, Science **296**, 712 (2002); F. De Martini, V. Bužek, F. Sciarrino, and C. Sias, Nature (London) **419**, 815 (2002).
[32] Z. Zhao, An-Ning Zhang, Xiao-Qi Zhou, Yu-Ao Chen, Chao-Yang Lu, Anders Karlsson, and Jian-Wei Pan, Phys. Rev. Lett. **95**, 030502 (2005).